Results in Physics 17 (2020) 103077

Contents lists available at ScienceDirect

Results in Physics

journal homepage: www.elsevier.com/locate/rinp

Design of dual-band polarization controllable metamaterial absorber at terahertz frequency

Ben-Xin Wang[a,*], Yuanhao He[a], Nianxi Xu[b], Xiaoyi Wang[b,*], Yanchao Wang[b], Jianjun Cao[a]

[a] School of Science, Jiangnan University, Wuxi 214122, China
[b] Key Laboratory of Optical System Advanced Manufacturing Technology, Changchun Institute of Optics, Fine Mechanics and Physics, Chinese Academy of Sciences, Changchun 130033, China

ARTICLE INFO

Keywords:
Metamaterials
Dual-band absorption
Polarization controllable
Terahertz

ABSTRACT

Dual-band polarization controllable terahertz metamaterial absorber consisting of two horizontal metallic strips and two vertically connected metallic strips is demonstrated. Due to different strip lengths in the two orthogonal directions, two near-perfect absorption peaks are firstly obtained when the incident beam electric field is in the horizontal direction, while two new peaks are next realized when the electric field is selected along the vertical direction. The near-field distributions in two specific directions are provided to investigate the mechanism of polarization controllable dual-band absorption. Our research should have broad application prospects in the selection, control and utilization of polarization-based devices.

Introduction

Considering the wide application prospects of metamaterial absorbers (MAs) in thermal emitters, solar cells, refractive-index sensing etc, we have witnessed their rapid development in the last decade [1–3]. The early MAs, however, usually have narrow-band absorption, which are not conducive to practical applications [1–5]. To maximum their potential in applications, multiple-band and broadband MAs have been wide-ranging demonstrated recently [6–25]. In fact, in addition to increasing the number of absorption peaks to expand practical applications, the polarization features of MAs are also a rather important index in evaluating the applications of absorption devices [11–25].

Regarding the polarization features, MAs usually have three types [11–20]. The first one is polarization insensitive MAs, whose absorption remain unchanged at any polarization. The second one is polarization sensitive MAs, which are only provide perfect absorption at a specific polarization. The third is polarization controllable (or dependent) MAs, which have completely different perfect absorption properties under two orthogonal polarization. A large number of literature studies have found that the first and second types of polarization features of MAs are extensively investigated because they are easy to realize by designing some highly symmetrical or asymmetrical top pattern structures [11–20]. Due to the mutual restriction and limitation of perfect absorption in two orthogonal directions, however, there are few reports on the MAs having the polarization controllable absorption performance.

Herein, a polarization controllable dual-band MA is designed. Its top structure consists of four metallic strips, of which two horizontal strips having the same and longer length, while the other two vertical strips have the same but shorter length. Two resonance peaks close to perfect absorption are realized when the incoming beam polarization is along the horizontal direction (X-polarization). Two new absorption peaks with an average absorbance of 97.28% can be achieved when the polarization is selected the vertical direction (Y-polarization). The mechanism of dual-band polarization controllable MA is studied by means of near-field distributions under the frequencies of maximum absorption peaks. In addition, polarization insensitive dual-band MA can be gained when the four metallic strips have the identical length.

Structure design and model

Fig. 1(a) and (b) give the structure sketch of dual-band polarization controllable MA. As revealed in Fig. 1(a), sandwich structure design of three functional layers is utilized for achieving the preset results. Its top structure in Fig. 1(b) is consisting of four metallic strips marked as A, B, C, and D. The four strips have the same width of $w = 10$ μm, while the lengths of them are different. The horizontal strips A and B have the same length $l_1 = 130$ μm, which is larger than that of vertical strips C and D having the same length $l_2 = 100$ μm, Distance between the vertical strip center (or horizontal strip center) and the basic cell center

* Corresponding authors.
E-mail addresses: wangbenxin@jiangnan.edu.cn (B.-X. Wang), wangxiaoyi@ciomp.ac.cn (X. Wang).

https://doi.org/10.1016/j.rinp.2020.103077
Received 22 February 2020; Received in revised form 24 March 2020; Accepted 24 March 2020
Available online 26 March 2020

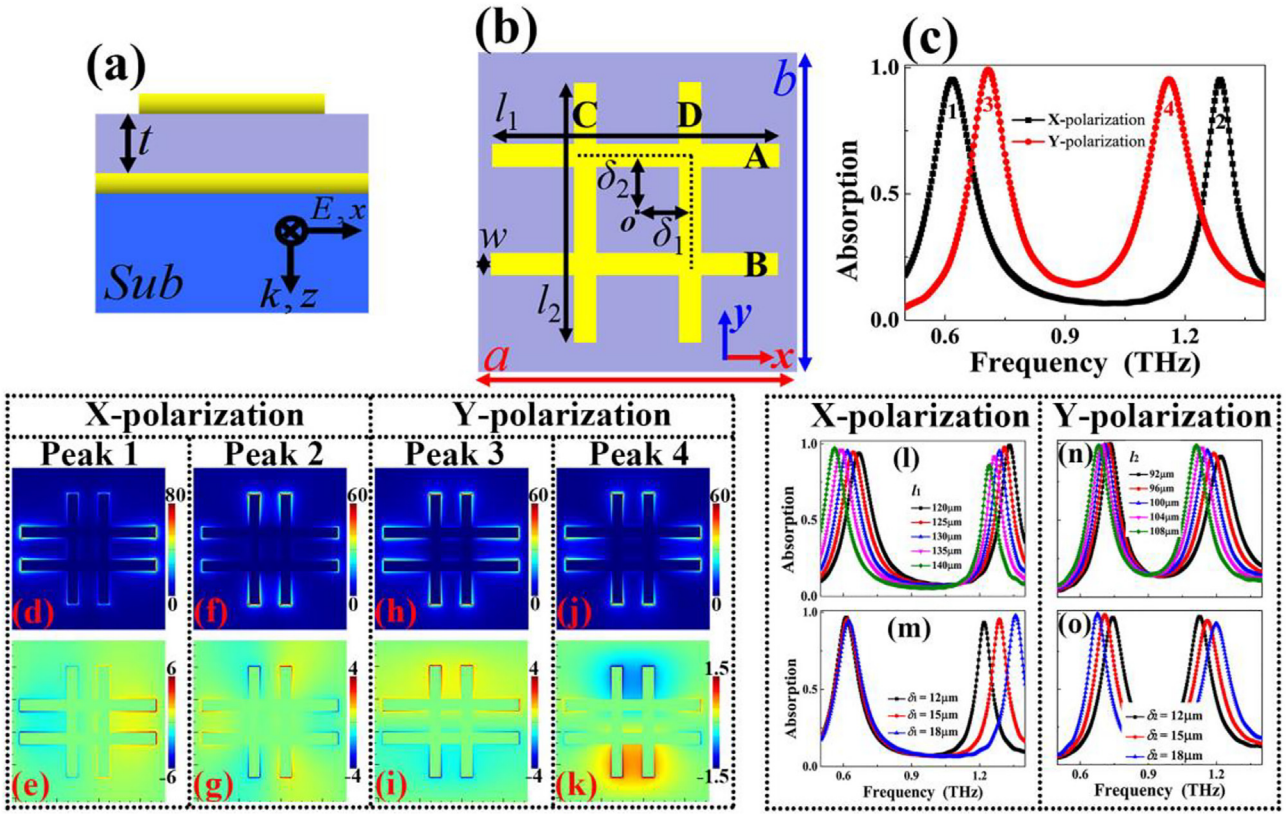

Fig. 1. (a) Side view of dual-band polarization controllable absorber; (b) Top view of dual-band polarization controllable absorber; (C) Absorption responses of the designed absorber under the X-polarization and Y-polarization; (d) and (f) are respectively the $|E|$ fields of the Peaks 1 and 2 under the X-polarization; (e) and (g) are respectively the *Ez* fields of the Peaks 1 and 2 under the X-polarization; (h) and (j) are respectively the $|E|$ fields of the Peaks 3 and 4 under the Y-polarization; (i) and (k) are respectively the *Ez* fields of the Peaks 3 and 4 under the Y-polarization; Dependence of absorption on the changes of the l_1 (l) and δ_1 (m) under the X-polarization; Dependence of absorption on the changes of the l2 (n) and δ_2 (o) under the Y-polarization.

o point is labeled as δ_1 (or δ_2), here $\delta_1 = \delta_2 = 15$ μm. For more details on structure design and model, please refer to the first section of Supplementary material.

Results and discussion

Fig. 1(c) shows the absorption under two orthogonal polarizations. Two absorption peaks having the frequencies of 0.62 THz (peak 1) and 1.29 THz (peak 2) are observed under X-polarization (horizontal direction), while two new absorption peaks 3 and 4 at frequencies of 0.71 THz and 1.16 THz can be obtained under Y-polarization (vertical direction), respectively. It is clear that the designed dual-band MA has the polarization controllable resonance response.

To reveal the physical cause of dual-band polarization adjustable absorption feature, near-field patterns under each specific polarization are given. We here first discuss the X-polarization case. The fields of peak 1 in Fig. 1(d) and (e) have similar characteristics that are mostly focused on both edges of horizontal strips, a very small proportion of fields can be found around the vertical strips. Moreover, its *Ez* field in Fig. 1(e) has opposite charges gathering at both edges of horizontal strips. These distribution features show that the peak 1 should be mainly due to dipole resonance of whole horizontal strips and has nothing to do with the existence of vertical strips. For peak 2, however, we observed that its $|E|$ field in Fig. 1(f) is not only concentrated at both edges of horizontal strips, but also at both edges of vertical strips. Its *Ez* field in Fig. 1(g) further indicates that two sets of opposite charges can be found. From these near-field patterns, it can be seen that the existence of vertical strips has an important role in forming the peak 2. The existence of vertical strips can divide the horizontal strips into several sections. The superposition of localized resonance response of these sections leads to the peak 2. According to the formation mechanism of peaks 1 and 2, it is easy to understand why the length l_1 changes of horizontal strips affect the resonance performance of the two peaks at the same time, see Fig. 1(l). Additionally, when the horizontal strip length remains unchanged and the position (δ_1) of vertical strips is changed, it can be predicted that the position changes (δ_1) of vertical strips can only affect the frequency of peak 2 without affecting (or slightly affecting) the peak 1 frequency. The results in Fig. 1(m) are in good agreement with this prediction.

Different from the near-field patterns of the peaks 1 and 2 under X-polarization, the near-field distributions of the peaks 3 and 4 under Y-polarization in Fig. 1(h)–(k) shows the same features that both edges of the four metallic strips have obvious field aggregation effects. In other words, the simultaneous existence and interaction of the horizontal strips and the vertical strips lead to the two peaks 3 and 4. This can explain why the length l_2 changes of the vertical strips and the position changes (δ_2) of the horizontal strips have obvious effect on the peaks 3 and 4, see Fig. 1(n) and (o). Due to different lengths of the four metallic strips in the horizontal and vertical directions, polarization controllable dual-band MA is obtained here. Dual-band polarization insensitive MA can be realized when the four metallic strips have the identical length in the two orthogonal directions (or highly symmetrical top pattern structure). Please see the second part of Supplementary material for detailed design of dual-band polarization insensitive MA

Compared with the existing technologies in obtaining the perfect absorption, the novelty or difference of manuscript is mainly reflected in the following aspects: (1) We pay attention to the research topic of polarization controllable which is often neglected in most of the reported literatures. The research on polarization controllable is mainly due to its more extensive application prospects compared with the

Table 1
Performance comparison between this work and the previous papers.

Reference	Polarization type	Sub-resonators number	Absorption mechanism	Frequency change way
7	Insensitive	5	Sub-resonator combination effect	Sub-resonator changes
8	Insensitive	4	Sub-resonator combination effect	Sub-resonator changes
9	Insensitive	4	Sub-resonator combination effect	Sub-resonator changes
10	Insensitive	13	Sub-resonator combination effect	Sub-resonator changes
11	Insensitive	6	Sub-resonator combination effect	Sub-resonator changes
12	Sensitive	3	Sub-resonator combination effect	Sub-resonator changes
13	Sensitive	4	Sub-resonator combination effect	Sub-resonator changes
14	Insensitive	25	Sub-resonator combination effect	Sub-resonator changes
15	Insensitive	4	Sub-resonator combination effect	Sub-resonator changes
16	Sensitive	9	Sub-resonator combination effect	Sub-resonator changes
This work	Controllable	1	Strong coupling between strips	Coupling intensity

absorption devices having the sensitive polarization or insensitive polarization. (2) Different from the existing technologies using a considerable number of sub-resonators to achieve multiple-band absorption, the proposed absorption device has the characteristics of simple structure design and easy to fabricate. (3) The physical mechanism of the absorption device is mainly due to the strong interaction of four metallic strips, which is obviously different from previous absorption devices that are caused by the superposition effect of the localized resonance response of each sub-resonator. (4) Considering the difference of absorption mechanism between this manuscript and previous absorption devices, the influence of structure parameters on absorption performance is also different. In addition, a tabular fashion in comparison to the state of the art literature for better visibility is also given, please the Table 1.

Conclusion

A new approach is provided to achieve the dual-band polarization controllable metamaterial absorber operated at terahertz domain using two horizontal strips and two vertically connected strips. Considering that the different strip lengths are in two orthogonal directions, a polarization controllable dual-band absorption performance is obtained. The mechanism of polarization controllable dual-band device is investigated using their near-field distributions in two specific directions. The results obtained here could have wide application prospects in the selection, control and utilization of polarization-based devices.

CRediT authorship contribution statement

Ben-Xin Wang: Conceptualization, Writing - review & editing, Software, Formal analysis, Methodology, Supervision, Funding acquisition. **Yuanhao He:** Data curation, Writing - original draft, Investigation. **Nianxi Xu:** Writing - original draft, Investigation. **Xiaoyi Wang:** Writing - original draft, Investigation. **Yanchao Wang:** Writing - original draft. **Jianjun Cao:** Writing - review & editing.

Acknowledgments

This research was funded by National Natural Science Foundation of China (11647143), Natural Science Foundation of Jiangsu (BK20160189), China Postdoctoral Science Foundation (2019M651692), Jiangsu Postdoctoral Science Foundation (2018K113C), Fundamental Research Funds for Central Universities (JUSRP51721B), Open Fund of Key Laboratory of Optical System Advanced Manufacturing Technology, Chinese Academy of Sciences (KLOMT190103).

Conflicts of interest

The authors declare no conflicts to declare.

Appendix A. Supplementary data

Supplementary data to this article can be found online at https://doi.org/10.1016/j.rinp.2020.103077.

References

[1] Landy NI, Sajuyigbe S, Mock JJ, Smith DR, Padilla WJ. Perfect metamaterial absorber. Phys Rev Lett 2008;100:207402.
[2] Liu N, Mesch M, Weiss T, Hentschel M, Giessen H. Infrared perfect absorber and its application as plasmonic sensor. Nano Lett 2010;10:2342.
[3] Liu X, Tyler T, Starr T, Starr AF, Jokerst NM, Padilla WJ. Taming the blackbody with infrared metamaterials as selective thermal emitters. Phys Rev Lett 2011;107:045901.
[4] Watts CM, Liu X, Padilla WJ. Metamaterial electromagnetic wave absorber. Adv Mater 2012;24:OP98.
[5] Cui Y, He Y, Jin Y, Ding F, Yang L, Ye Y, et al. Plasmonic and metamaterial structures as electromagnetic absorbers. Laser Photon Rev 2014;8:495.
[6] Yu P, Besteiro LV, Huang Y, Wu J, Fu L, Tan HH, et al. Broadband metamaterial absorbers. Adv Opt Mater 2019;7:1800995.
[7] Yuan S, Yang R, Xu J, Wang J, Tian J. Photoexcited switchable single-/dual-band terahertz metamaterial absorber. Mater Res Express 2019;6:075807.
[8] Zhao L, Liu H, He Z, Dong S. Theoretical design of twelve-band infrared metamaterial perfect absorber by combining the dipole, quadrupole, and octopole plasmon resonance modes of four different ring-strip resonators. Opt Express 2018;26:12838.
[9] Khuyen BX, Tung BS, Kim YJ, Hwang JS, Kim KW, Rhee JY, et al. Ultra-subwavelength thickness for dual/triple-band metamaterial absorber at very low frequency. Sci Rep 2018;8:11632.
[10] Jafari FS, Naderi M, Hatami A, Zarrabi FB. Microwave Jerusalem cross absorber by metamaterial split ring resonator load to obtain polarization independence with triple band application. Int J Electron Commun 2019;101:138.
[11] Mao Q, Feng C, Yang Y, Tan Y. Design of broadband metamaterial near-perfect absorbers in visible region based on stacked metal-dielectric gratings. Mater Res Express 2018;5:065801.
[12] Wang BX, Tang C, Niu Q, He Y, Chen T. Design of narrow discrete distances of dual-/triple-band terahertz metamaterial absorbers. Nanoscale Res Lett 2019;14:64.
[13] Tran CM, Pham HV, Nguyen HT, Nguyen TT, Vu LD, Do TH. Creating multiband and broadband metamaterial absorber by multiporous square layer structure. Plasmonics 2019;14:1587.
[14] Chen W, Chen R, Zhou Y, Ma Y. Broadband metamaterial absorber with an in-band metasurface function. Opt Lett 2019;44:1076.
[15] Liu S, Zhuge J, Ma S, Chen H, Bao D, He Q, et al. A bi-layered quad-band metamaterial absorber at terahertz frequencies. J Appl Phys 2016;118:245304.
[16] Liu S, Chen H, Cui TJ. A broadband terahertz absorber using multi-layer stacked bars. Appl Phys Lett 2015;106:151601.
[17] Wang BX, He Y, Lou P, Xing W. Design of dual-band terahertz metamaterial absorber using two identical square patches for sensing application. Nanoscale Adv 2020;2:763.
[18] Wang BX, He Y, Lou P, Huang WQ, Pi F. Penta-band terahertz light absorber using five localized resonance responses of three patterned resonators. Results Phys 2020;16:102930.
[19] Wang BX, Wang GZ, Sang T. Simple design of novel triple-band terahertz metamaterial absorber for sensing application. J Phys D 2016;49:165307.
[20] Wang BX, Wang GZ, Wang LL. Design of a novel dual-band terahertz metamaterial absorber. Plasmonics 2016;11:523.
[21] Wang BX. Quad-band terahertz metamaterial absorber based on the combining of the dipole and quadrupole resonances of two SRRs. IEEE J Sel Top Quant Electron 2017;23:4700107.
[22] Wang BX, Wang GZ, Sang T, Wang LL. Six-band terahertz metamaterial absorber based on the combination of multiple-order responses of metallic patches in a dual-layer stacked resonance structure. Sci Rep 2017;7:41373.
[23] Ghosh SK, Yadav VS, Das S, Bhattacharyya S. Tunable graphene based metasurface for polarization-independent broadband absorption in lower mid infrared (MIR) range. IEEE Trans Electromagn Compatibility. doi:10.1109/TEMC.2019.2900757.
[24] Nilotpal, Nama L, Bhattacharyya S, Chakrabarti P. A metasurface-based broadband quasi non-dispersive cross polarization converter for infrared region. Wiley Int J RF Microwave Comput Aided Eng 2019;29:e21889.
[25] Yadav VS, Ghosh SK, Das S, Bhattacharyya S. Wideband tunable mid-infrared cross-polarization converter using monolayered graphene-based metasurface over a wide angel of incidence. IET Microwaves Antennas Propag 2019;13:82.